

# Negative and zero thermal expansion in $\alpha$ - (Cu<sub>2-x</sub>Zn<sub>x</sub>)V<sub>2</sub>O<sub>7</sub> solid solutions

Naike Shi<sup>1</sup>, Andrea Sanson<sup>2</sup>, Alessandro Venier<sup>2</sup>, Longlong Fan<sup>3,4</sup>, Chengjun Sun<sup>4</sup>,  
Xianran Xing<sup>1</sup> & Jun Chen<sup>1\*</sup>

<sup>1</sup> *Beijing Advanced Innovation Center for Materials Genome Engineering, and Department of Physical Chemistry, University of Science and Technology Beijing, Beijing 100083, China.*

<sup>2</sup> *Department of Physics and Astronomy, University of Padova, Padova I-35131, Italy*

<sup>3</sup> *College of Physics and Materials Science, Tianjin Normal University, Tianjin 300387, China*

<sup>4</sup> *Argonne National Laboratory, X-ray Science Division, Argonne, Illinois 60439, United States*

Correspondence and requests for materials should be addressed to Jun Chen (email: [junchen@ustb.edu.cn](mailto:junchen@ustb.edu.cn)).

## 1. Experiment and data analysis details

The samples of  $\alpha$ -Cu<sub>2-x</sub>Zn<sub>x</sub>V<sub>2</sub>O<sub>7</sub> ( $x = 0, 0.1, 0.2$ ) solid solutions were prepared by a solid-state reaction method. The stoichiometric precursors of CuO, ZnO, and V<sub>2</sub>O<sub>5</sub> were mixed gently and grounded in an agate mortar with appropriate amount of anhydrous alcohol for 30min. Then the mixture was heated at 373K in air for one hour to remove water. The dried powder was pressed into a pellet of  $\phi 8 \times 4$  mm under the pressure of 10MPa by a tableting machine. The pellet was heated with the heating rate of 5K/min, and sintered at 873K for 3 hours. After that, the sample was cooled naturally and grounded into powder. Finally, the pure  $\alpha$ -Cu<sub>2-x</sub>Zn<sub>x</sub>V<sub>2</sub>O<sub>7</sub> sample was obtained.

Crystal structure and thermal expansion properties were investigated by temperature dependence of powder X-ray diffraction (PXRD) at laboratory (PW3040/60, PANalytical) and high-resolution synchrotron X-ray diffraction (SXRD) ( $\lambda = 0.412634 \text{ \AA}$ ) at the beamline 11-BM-B of APS (Argonne National Laboratory, USA). The crystal structure was refined by the Rietveld method using FULLPROF software based on an orthorhombic (*Fdd2*) model.

The Cu K-edge and V K-edge of EXAFS measurements were performed in  $\alpha$ -Cu<sub>2</sub>V<sub>2</sub>O<sub>7</sub> from 148 K to 498 K with a step of 50 K at the 20-BM-B beamline of APS according to the well-established procedures<sup>1</sup>. The samples for EXAFS were prepared by mixing and pelletizing the samples powder with boron nitride powder. The amount of sample powder was chosen to have an absorption edge jump  $\Delta\mu_x \sim 1$ . The EXAFS spectra were collected in transmission mode in the energy range  $\sim 8.7$ -10.1 keV for Cu K-edge and  $\sim 5.2$ -6.6 keV for V K-edge respectively, using a Si (111) double-crystal monochromator, with an energy step varying from 0.2 eV in the near-edge region to about 4 eV at the highest energies, thus to obtain a uniform wave vector step  $\Delta k \sim 0.035 \text{ \AA}^{-1}$ . The sample was mounted in a nitrogen cryostat / heater oven. The temperature was stabilized and monitored using an electric heater controlled by a feedback loop, ensuring a thermal stability within  $\pm 1$  K. Two spectra were collected at each temperature point.

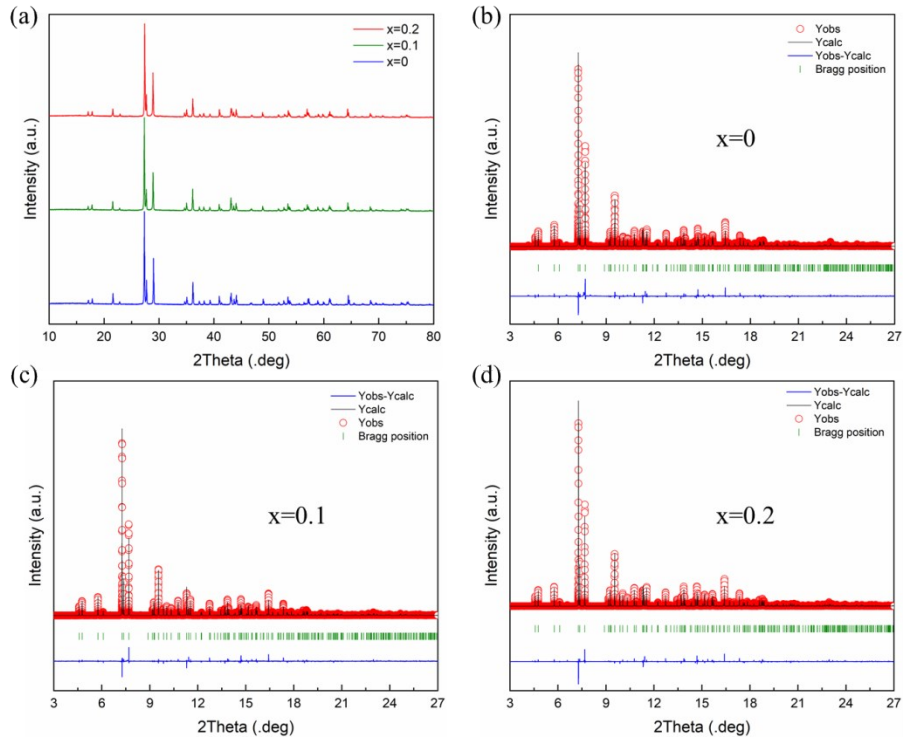


**Figure S1.** (a) PXR spectra, and (b), (c), (d) SXR refinements of  $\alpha\text{-Cu}_{2-x}\text{Zn}_x\text{V}_2\text{O}_7$  ( $x = 0, 0.1, 0.2$ ) at room temperature.

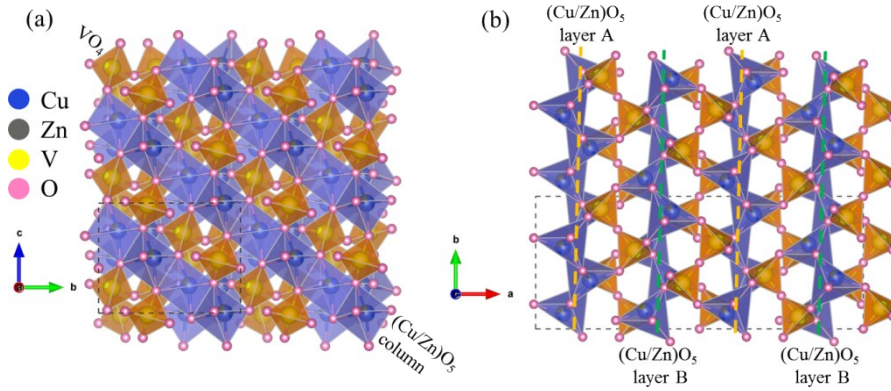


**Figure S2.** Crystal structure of  $\alpha\text{-Cu}_{2-x}\text{Zn}_x\text{V}_2\text{O}_7$  ( $x = 0, 0.1, 0.2$ ).

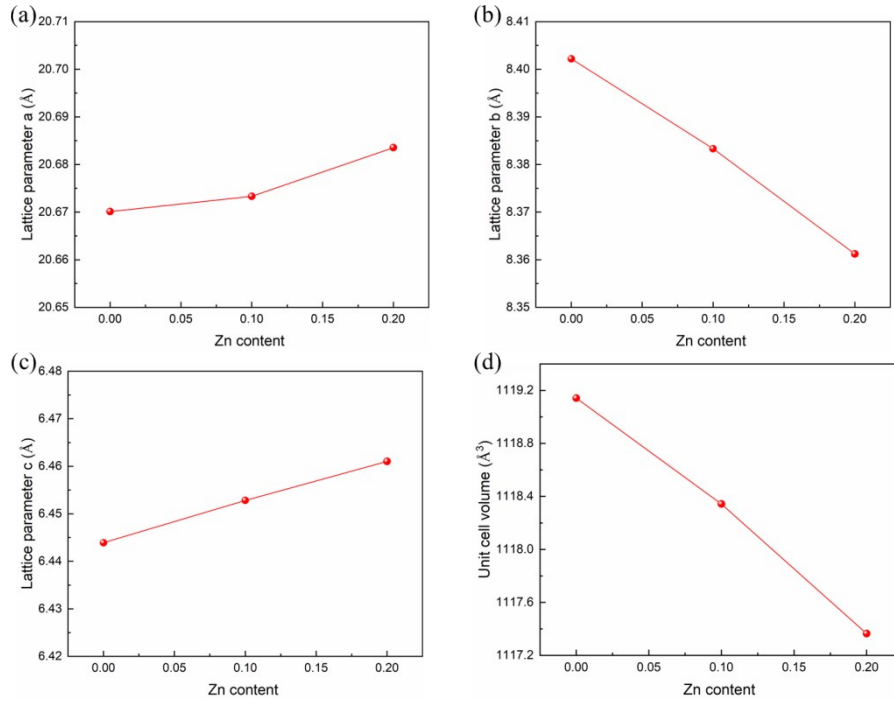


**Figure S3.** Lattice parameters of  $\alpha$ - $\text{Cu}_{2-x}\text{Zn}_x\text{V}_2\text{O}_7$  as a function of Zn content.

**Table S1.** CTE in different directions of  $\alpha$ - $\text{Cu}_{2-x}\text{Zn}_x\text{V}_2\text{O}_7$  ( $x = 0, 0.1, 0.2$ ).

	$x = 0$	$x = 0.1$	$x = 0.2$
$\alpha_a$ ( $\times 10^{-6} \text{ K}^{-1}$ )	1.50	3.13	2.27
$\alpha_b$ ( $\times 10^{-6} \text{ K}^{-1}$ )	-17.44	-16.30	-8.58
$\alpha_c$ ( $\times 10^{-6} \text{ K}^{-1}$ )	5.80	5.33	4.74
$\alpha_V$ ( $\times 10^{-6} \text{ K}^{-1}$ )	-10.19	-7.89	-1.58

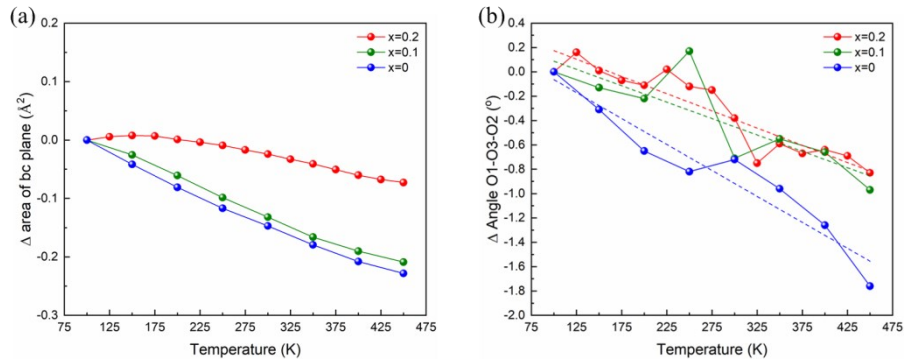


**Figure S4.** Temperature dependence of (a) the area of  $bc$  plane, and (b) the angle  $\text{O1-O3-O2}$

O3-O2 ( $\gamma$ , shown in Figure 2a).

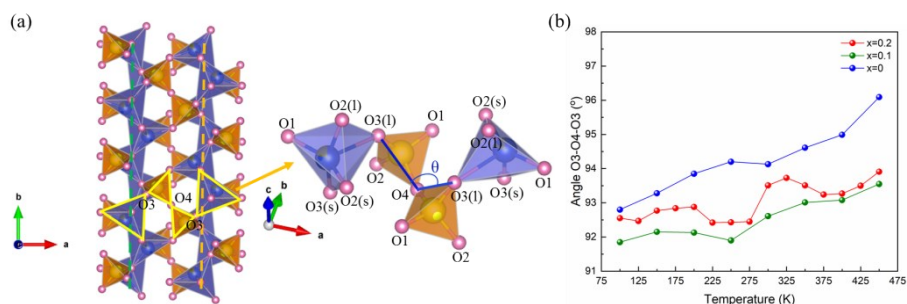


**Figure S5.** (a) Diagram of  $(\text{Cu/Zn})\text{O}_5$  layers from the view of  $c$  axis. (b) The angle O3-O4-O3 ( $\theta$ ) as a function of temperature.

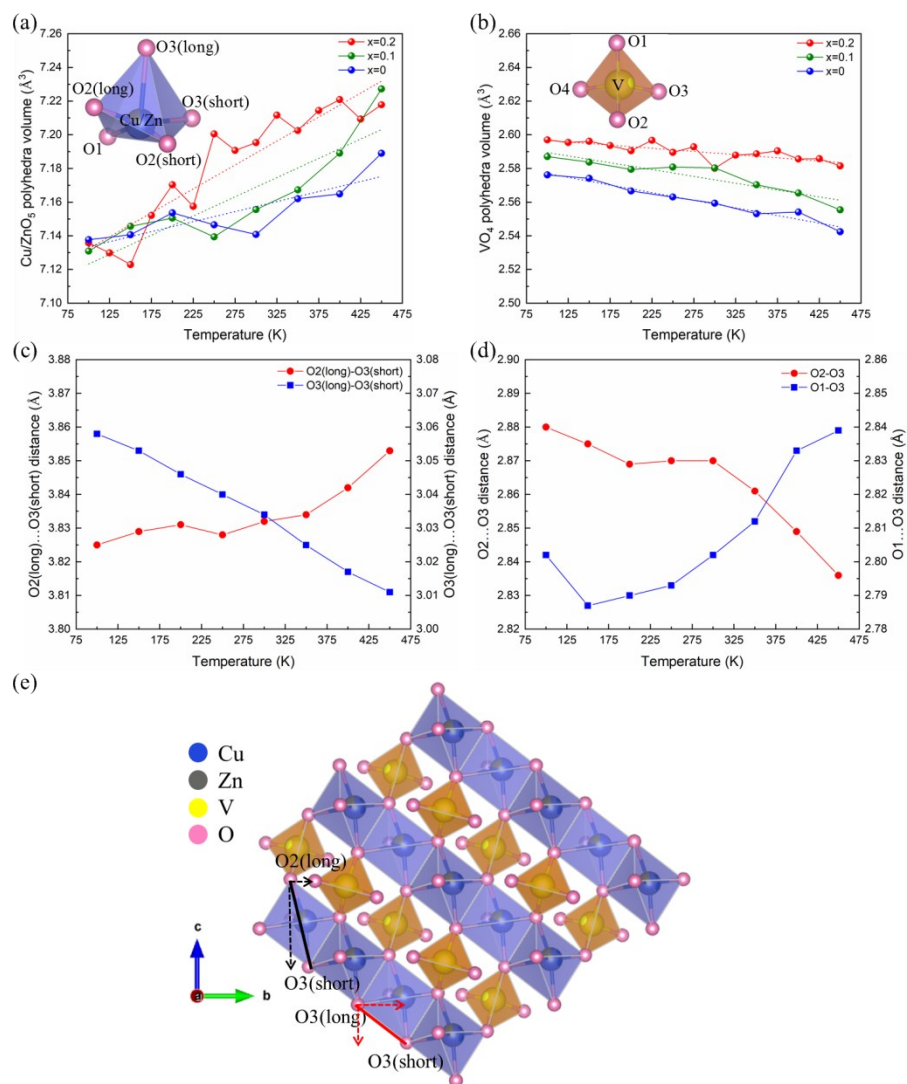


**Figure S6.** Temperature dependence of (a)  $(\text{Cu/Zn})\text{O}_5$  volume and (b)  $\text{VO}_4$  volume in  $\alpha\text{-Cu}_{2-x}\text{Zn}_x\text{V}_2\text{O}_7$  ( $x = 0, 0.1, 0.2$ ). The insets are illustrations of  $(\text{Cu/Zn})\text{O}_5$  and  $\text{VO}_4$

polyhedra. (c) The edge lengths of O3(long)-O3(short) and O2(long)-O3(short) in the CuO<sub>5</sub> quadrangular pyramid, and (d) the O1-O3 and O2-O3 edge lengths in VO<sub>4</sub> tetrahedra as a function of temperature. (e) The illustration of crystal structure in a single (Cu/Zn)O<sub>5</sub> layer from the view of the axis *a*. It can be seen that the increasing length of O2(long)-O3(short) (the dark line) in CuO<sub>5</sub> has a much larger component along the *c*-axis than the *b*-axis (dark dotted lines), while the shrinkage of O3(long)-O3(short) (the red line) has an equal components on the *b* and *c* axes (red dotted lines).

**Table S2.** Scattering paths related to the 1st peak of the FT structure of Cu<sub>2</sub>V<sub>2</sub>O<sub>7</sub> calculated by FEFF code<sup>2</sup>, correspond to single scattering from the first Cu-O coordination shell. The last column lists the fitting parameters (distance, Debye-Waller factor, and third cumulants).

Index	Path	Legs	Degeneracy	reff (Å)	Amplitude	Parameters
1	Cu-O1	2	1	1.8820	100.00	$r_1, \sigma_1^2, C_3$
2	Cu-O2	2	1	1.9328	93.68	
3	Cu-O3	2	1	1.9515	91.49	
4	Cu-O4	2	1	1.9671	89.73	
5	Cu-O5	2	1	2.5326	47.880	Neglected

**Table S3.** Scattering paths related to the FT structure between about 0.5 and 2.0 Å of Cu<sub>2</sub>V<sub>2</sub>O<sub>7</sub> calculated by FEFF code<sup>2</sup>, correspond to single scattering from the first V-O coordination shell. The last column lists the fitting parameters (distance and Debye-Waller factor). The fitting parameters have reduced as much possible to stabilize the fitting

Index	Path	Legs	Degeneracy	reff (Å)	Amplitude	Parameters
1	V-O1	2	1	1.6251	100.00	$r_1, \sigma_1^2, C_3$
2	V-O2	2	1	1.6899	91.20	
3	V-O3	2	1	1.7368	85.49	
4	V-O4	2	1	1.8061	77.96	

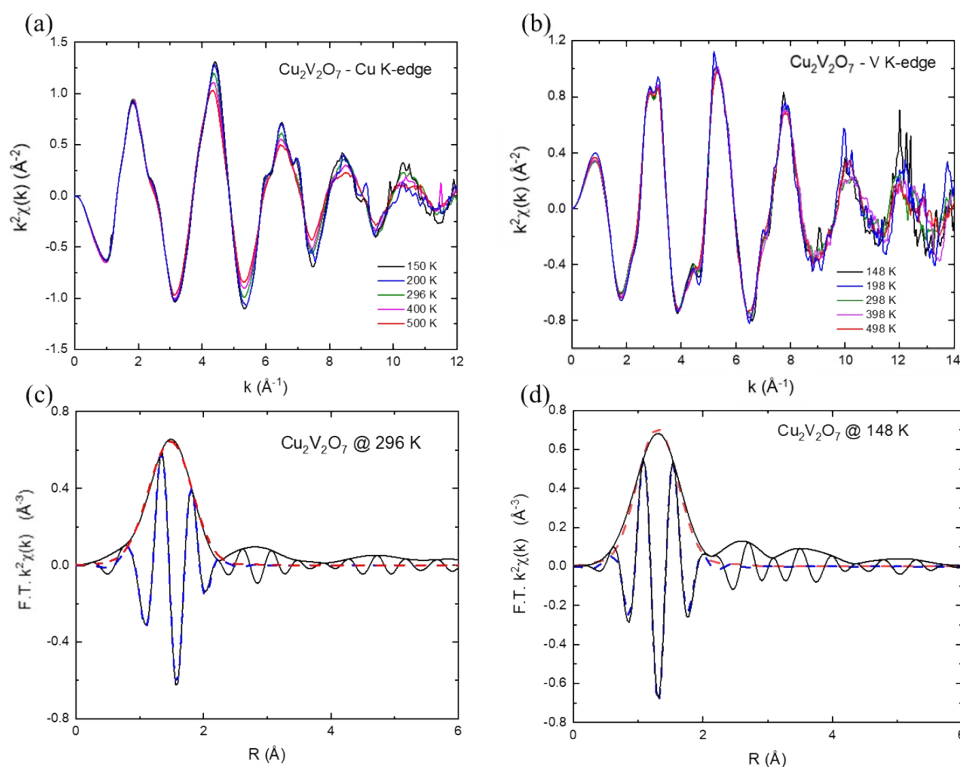


**Figure S7.** (a)  $k^2$ -weighted EXAFS signal of Cu K-edge and (b) V K-edge of  $\text{Cu}_2\text{V}_2\text{O}_7$  as a function of temperature. (c) Modulus and imaginary part of the Fourier transform of the Cu K-edge EXAFS signal (continuous lines) and example of best-fitting simulation of the first peak (dashed-bold lines) at 296K, and (d) Modulus and imaginary part of the Fourier transform of the V K-edge EXAFS signal (continuous lines) and example of best-fitting simulation of the first peak (dashed-bold lines) at 148K performed by using the FEFFIT package<sup>3</sup>.

**Table S4.** Comparison between the vibrational parameters of the Cu-O and V-O atomic pairs in  $\text{Cu}_2\text{V}_2\text{O}_7$ .  $\nu_{\parallel}$  and  $\nu_{\perp}$  are the best-fitting Einstein frequencies of the parallel and perpendicular MSRDS, respectively;  $k_{\parallel}$  and  $k_{\perp}$  are the corresponding bond-stretching and bond-bending effective force constants,  $\gamma$  represents the anisotropy of the relative thermal vibrations.

	<b>Cu<sub>2</sub>V<sub>2</sub>O<sub>7</sub></b>
<b>Cu-O stretching</b>	$\nu_{\parallel} = 11.98 \pm 0.55 \text{ THz}$ $k_{\parallel} = 7.50 \pm 0.69 \text{ eV/\AA}^2$
<b>V-O stretching</b>	$\nu_{\parallel} = 15.03 \pm 1.33 \text{ THz}$ $k_{\parallel} = 11.3 \pm 2.0 \text{ eV/\AA}^2$
<b>Cu-O bending</b>	$\nu_{\perp} = 7.06 \pm 1.13 \text{ THz}$ $k_{\perp} = 2.61 \pm 0.83 \text{ eV/\AA}^2$
<b>V-O bending</b>	$\nu_{\perp} = 4.95 \pm 0.31 \text{ THz}$ $k_{\perp} = 1.22 \pm 0.15 \text{ eV/\AA}^2$
<b>Cu-O anisotropy at 300 K</b>	$\gamma \sim 4.9 \pm 2.5$
<b>V-O anisotropy at 300 K</b>	$\gamma \sim 13.5 \pm 2.8$

## Reference

1 (a) Sayers, D. E.; Bunker, B. A. in X-ray Absorption: Principles, Applications, Techniques of EXAFS, SEXAFS and XANES, edited by Koningsberger D. C. and Prins R. (Wiley, New York, 1988). (b) Fornasini, P. in Synchrotron Radiation - Basics, Methods and Applications, edited by Mobilio, S.; Meneghini, C.; Boscherini, F. (Springer-Verlag, Berlin, 2015), Chap. 6, pp. 181–211.

2 L. Ankudinov, B. Ravel, J. J. Rehr and S. D. Conradson, *Phys. Rev. B*, 1998, **58**, 7565.

3 M. Newville, B. Ravel, J. J. Rehr, E. Stern and Y. Yacoby, *Physica. B*, 1995, **208**, 154.